Isoelectronic studies of the $5s^2\,^1S_0$–$5s5p\,^{1,3}P_J$ intervals in the Cd sequence

Lorenzo J. Curtis

Department of Physics and Astronomy, University of Toledo, Toledo, Ohio 43606

The $5s^2\,^1S_0$–$5s5p\,^{1,3}P_J$ energy intervals in the Cd isoelectronic sequence have been investigated through a semiempirical systematization of recent measurements and through the performance of *ab initio* multiconfiguration Dirac–Fock calculations. Screening-parameter reductions of the spin–orbit and exchange energies both for the observed data and for the theoretically computed values establish the existence of empirical linearities similar to those exploited earlier for the Be, Mg, and Zn sequences. This permits extrapolative isoelectronic predictions of the relative energies of the $5s5p$ levels, which can be connected to $5s^2$ using intersinglet intervals obtained from empirically corrected *ab initio* calculations. These linearities have also been examined homologously for the Zn, Cd, and Hg sequences, and common relationships have been found that accurately describe all three of these sequences.

INTRODUCTION

Energy levels of ns^2 and $nsnp$ configurations in two valence electron isoelectronic systems have recently been the object of a number of experimental and calculational studies. Intraterm and spin intercombination transitions among these levels become relatively stronger with increasing nuclear charge, and corresponding radiative emissions from highly ionized members of these sequences have been observed in high-temperature plasmas. Since these lines are often isolated and in a conveniently detectable wavelength region, they can provide useful diagnostic probes.

Semiempirical systematizations of the existing data have been made for the $n = 2$ Be,[1] $n = 3$ Mg,[2] and $n = 4$ Zn (Ref. 3) sequences using screening parameterization methods, which have revealed linearities that permit reliable interpolative and extrapolative predictions. Data near the neutral end of the homologous $n = 5$ Cd sequence showed similar trends,[4] but it was only recently that observations to moderate stages of ionization for this sequence have been carried out.[5] In the study reported herein I have supplemented the observed data with multiconfiguration Dirac–Fock *ab initio* theoretical calculations to high stages of ionization and have made screening parameter reductions of both the existing experimental data and the theoretical calculations. This formulation has permitted me to verify the persistence to $n = 5$ of the linearities noted earlier for the $n = 2, 3$, and 4 sequences and to make reliable extrapolative predictions of the $5s^2$–$5s5p$ intervals. I have also studied the homologous behavior of the system and found that a set of reduced screening parameters can be defined through which the ns^2–$nsnp$ intervals in the Zn, Cd, and Hg sequences are accurately described by common linear relationships.

EXPERIMENTAL DATA BASE

Recently Kaufman and Sugar[5] performed measurements of the $5s5p\,^3P_0$, $^3P_1$, $^3P_2$, and $^1P_1$ excitation energies for the Cd-like ions I^{+5}, Xe^{+6}, Cs^{+7}, Ba^{+8}, and La^{+9}. Before these

measurements the data base consisted of the values for neutral Cd through Te^{+4} listed in the 1948 compilation of Moore[6] with confirming remeasurements in neutral Cd (Ref. 7) and Te^{+4},[8] and measurements in I^{+5} (Ref. 9) and Xe^{+6} (Ref. 10) (now superseded by Ref. 5). Since semiempirical linearizations must usually exclude ions near the neutral end of an isoelectronic sequence (where the validity of the central field approximation weakens) a reliable analysis of this type has become possible only by virtue of the studies by Kaufman and Sugar.[5] The available data base with source references is given in Table 1. Despite the increasing validity of jj coupling in extrapolations to higher stages of ionization, LS coupling notation will be used here to label the energy eigenstates, with the understanding that the spin designation is only identificational.

In earlier studies of the Mg and Zn sequences, experimental measurements extended to much higher stages of ionization for the $ns^2\,^1S_0$–$nsnp\,^1P_1$ resonance transition than for the intercombination line and intratriplet intervals, and predictions for all ns^2–$nsnp$ intervals could be made through a semiempirical specification of the relative positions within the $nsnp$ configuration. As shown in Table 1, neither the singlet nor triplet levels have been observed for the Cd sequence for ionization stages greater than 10, which necessitates the combined semiempirical and *ab initio* approach used here.

MULTICONFIGURATION DIRAC–FOCK CALCULATIONS

To compare the empirical trends revealed by the semiempirical formulation with the predictions of existing *ab initio* theories, extensive calculations were performed as part of this study using a multiconfiguration Dirac–Fock code. Calculations were carried out by network on the National Magnetic Fusion Center CRAY X-MP E computer and required approximately 90 min of CPU time. The code is an improved second version[11] of the program MCDF developed by Grant and co-workers.[12] The relativistic multiconfigura-

Table 1. The Experimental Data Base with Source References, Together with the Results of the Multiconfiguration Dirac–Fock Calculation (in cm^{-1})

Z	Ion	$^1S_0$–$^3P_0$ Obs.	$^1S_0$–$^3P_0$ MCDF	$^1S_0$–$^3P_1$ Obs.	$^1S_0$–$^3P_1$ MCDF	$^1S_0$–$^3P_2$ Obs.	$^1S_0$–$^3P_2$ MCDF	$^1S_0$–$^1P_1$ Obs.	$^1S_0$–$^1P_1$ MCDF	Obs. Ref.
48	Cd	30 114	—	30 656	—	31 827	—	43 692	—	7
49	In+1	42 275	—	43 349	—	45 827	—	63 034	—	6
50	Sn+2	53 548	—	55 196	—	59 229	—	79 911	—	6
51	Sb+3	64 435	—	66 700	—	72 560	—	95 952	—	6
52	Te+4	75 110	69 231	78 025	72 315	86 006	79 790	111 708	115 576	8
53	I+5	85 666	79 875	89 262	83 732	99 686	93 488	127 424	131 902	5
54	Xe+6	96 140	90 375	100 451	95 026	113 673	107 440	143 261	148 224	5
55	Cs+7	106 570	100 779	111 630	106 235	128 031	121 702	159 326	164 670	5
56	Ba+8	116 984	111 131	122 812	117 419	142 805	136 347	175 711	181 363	5
57	La+9	127 413	121 464	134 019	128 620	158 084	151 444	192 481	198 402	5
58	Ce+10		131 805		139 864		167 053	209 808	215 866	5
59	Pr+11		142 176		151 175		183 230		233 823	
60	Nd+12		152 608		162 580		200 041		252 348	
61	Pm+13		163 176		174 148		217 594		271 555	
62	Sm+14		174 363		186 361		236 410		291 967	
63	Eu+15		181 799		194 842		252 155		309 245	
64	Gd+16		193 645		207 750		273 033		331 574	
65	Tb+17		204 475		219 654		293 657		353 514	
66	Dy+18		215 240		231 498		315 021		375 855	
67	Ho+19		226 033		243 366		337 260		396 616	
68	Er+20		236 877		255 258		360 396		433 716	
69	Tm+21		247 775		267 083		384 831		453 713	
70	Yb+22		258 669		274 536		410 064		479 635	
71	Lu+23		271 040		287 916		436 495		507 232	
72	Hf+24		281 339		304 950		464 128		536 181	
73	Ta+25		292 537		317 139		493 027		566 460	
74	W+26		303 883		329 574		523 251		598 098	
82	Pb+34		398 712		433 612		821 483		907 985	
92	U+44		528 446		575 171		1 386 786		1 487 865	

tion self-consistent field calculation included the $5s^2$, $5p^2$, $5d^2$, $4f^2$, $5s5p$, $5p5d$, and $4f5d$ configurations. Studies were also made of the $4f$ ionization limit. Perturbative corrections were included to account for the finite size of the nucleus and the Breit interaction, as well as vacuum polarization, electron self-energy, and other quantum electrodynamic effects.

To obtain convergence the calculations were begun at U^{+44} and successively stepped to lower Z, using the preceding wave functions as starting values. Convergence became more difficult near the neutral end of the sequence, but discrepencies with experiment also increased there, and calculations were terminated at Te^{+4}. Calculations are thus reported for all elements from Te^{+4} through W^{+26}, as well as for Pb^{+34} and U^{+44}.

The isoelectronic behavior of the important interacting configurations is shown in Fig. 1, and the calculations for the $5s^2$–$5s5p$ intervals are juxtiposed with the available experimental data in Table 1. There are large but systematic discrepencies between raw theoretical calculations and experiment. For the $5s5p$ configuration, the MCDF calculations overestimate the singlet excitation energy by about 3%, overestimate the singlet–triplet splitting by about 20%, and underestimate the $J = 0$–2 fine structure by about 3%. Thus it is necessary to invoke semiempirical methods to attain the accuracies required for spectroscopic classification work. These methods are described in the next section.

SCREENING PARAMETER FORMULATION

The goal of the systematization is to reduce the three energy intervals between the $^3P_0$ $^3P_1$, $^3P_2$, and $^1P_1$ levels to an alternative set of three quantities that contain the same information but have a simpler and more slowly varying dependence on Z. The approach is the same as was described in Ref. 3 and utilizes the intermediate coupling equations connecting the $nsnp$ singlet and triplet levels. Although these equa-
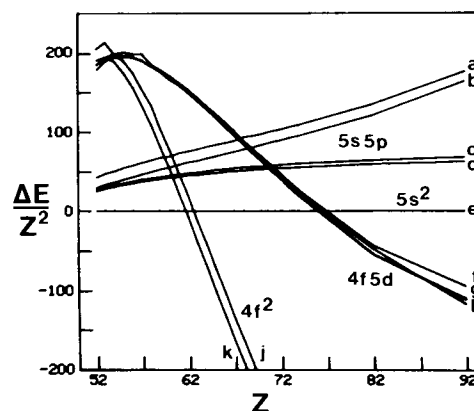

Fig. 1. MCDF energies of selected levels relative to $5s^2$ ^1S, scaled to Z^2 and plotted versus Z (in reciprocal centimeters). The curves are labeled as follows: a is $5s5p$ $^1P_1$; b, c, and d are $5s5p$ $^3P_{2,1,0}$; e is $5s^2$ $^1S_0$; f is $5d5f$ $^1P_0$; g, h, and i are $5d5f$ $^3P_{2,1,0}$; j is $4f^2$ $^3H_4$; k is $4f^2$ $^1S_0$.

Table 2. Slater Exchange Energies Computed from Exact Hydrogenic Wave Functions (in Rydberg Units)[a]

Config.	Seq.	$G_1(H)/R$	Decimal Equivalent	A(Edlén)/R
2s2p	Be	$2^{-8} * 3 * 5$	0.0586	0.0586[b]
3s3p	Mg	$2^{-8} * 3^{-2} * 5 * 13$	0.0282	0.0271
4s4p	Zn	$2^{-18} * 3^2 * 5^2 * 19$	0.0163	0.0176
5s5p	Cd	$2^{-27} * 3^{-5} * 5^{-5} * 11$ $* 233 * 420\,286\,277$	0.0106	0.0101
6s6p	Hg	$2^{-21} * 3^{-9} * 5^{-3} * 7^{-1} * 29$ $* 191 * 48\,186\,107$	0.0074	0.0085

[a] The computations are compared with empirical fits by Edlén.[4]
[b] Calculated.

tions involve only two quantities, the spin–orbit energy ζ and the exchange Slater energy G_1, a third quantity can be introduced by independently determining G_1 from two different singlet–triplet intervals. The reduction is thus defined by the equations

$$^3P_2 - {}^3P_0 = 3\zeta/2, \tag{1}$$

$$^1P_1 - {}^3P_2 = G_{1A} - 3\zeta/4 + [(G_{1A} + \zeta/4)^2 + \zeta^2/2]^{1/2}, \tag{2}$$

$$^1P_1 - {}^3P_1 = 2[(G_{1B} + \zeta/4)^2 + \zeta^2/2]^{1/2}. \tag{3}$$

In practice, G_{1A} and G_{1B} are nearly the same, but their separate determination relaxes the assumption of exact validity for the intermediate coupling equations. When measured energy intervals are reduced to the corresponding values for ζ, G_{1A}, and G_{1B}, it is empirically observed that the quantities obey simpler charge scaling laws than do the raw energies, and the charge dependences can be linearized by appropriate screening parameterizations.

A screened Sommerfeld–Dirac expansion is used to parameterize ζ:

$$\zeta = R\alpha^2(Z - S_\zeta)^4/3n^2 + \text{higher order}. \tag{4}$$

Here R is the reduced-mass-corrected Rydberg constant, α is the fine-structure constant, Z is the nuclear charge, and S_ζ denotes the empirical screening parameter that Eq. (4) serves to define. The higher-order terms in Eq. (4) include additional contributions to the Dirac energy and radiative corrections that have been described in detail elsewhere.[2,3]

The exchange Slater energy can be parameterized using the expression for the corresponding quantity calculated using screened hydrogenlike wave functions. If the ns and np electrons are described by the same effective central charge, the hydrogenic calculation is linear in that central charge, with a proportionality constant $G_n{}^H$ that is an n-dependent rational fraction multiplied by R. Thus the parameterization used herein was defined through the equation

$$G_1 = G_n{}^H(Z - S_G)/(1 - \epsilon). \tag{5}$$

Here ϵ is an additional fitting parameter, a small correction introduced to optimize the isoelectronic regularity. Values for $G_n{}^H$ for the $nsnp$ systems were explicitly calculated and are presented as ratios of prime numbers in Table 2. Although the accuracy of this presentation greatly exceeds our needs, it is used to emphasize the role of S_G and ϵ as devi-

ation indices from an idealized hydrogenic model. (The very large primes occur because of a subtraction between products and quotients of lower primes inherent in the incomplete gamma functions, and these results thus differ for $n \geq 4$ from seven-figure rationlizations used earlier.[2])

The three measured energy intervals can thus be re-expressed as the three screening parameters S_ζ, S_{GA}, and S_{GB}. When measured data are reduced to these effective screening parameters, their isoelectronic behavior is often[1-4] well represented by the ansatz

$$S_i = a_i + b_i/(Z - S_i), \tag{6}$$

which permits extrapolative predictions.

It is interesting to note that Eqs. (5) and (6) were applied as early as 1964 to the data then available for n = 2–6 by Edlén (Ref. 4, p. 171). Edlén computed $G_2{}^H$ theoretically but evaluated $G_n{}^H$ for n = 3–6 empirically. His results are compared in Table 2 with the rational fractions obtained from our hydrogenic calculations and are in close agreement.

RESULTS

The MCDF calculations quantified a number of features of this isoelectronic sequence, which are illustrated in Fig. 1. In this plot various relativistic energy levels are selected and labeled according to their dominant nonrelativistic configuration amplitude, scaled to Z^2, and traced isoelectronically. The $5s^2\,{}^1S_0$ (e) ceases to be the lowest-lying level between Z = 61 and 62, where it is replaced as the ground state by the $4f^2\,{}^3H_4$ level (k). Thus, for $Z > 62$, this work is properly a study of the two lowest-lying doubly excited levels in the Cd sequence. However, calculations of the singly excited $4f\,{}^2F$ ionization potential indicate that the doubly excited $5s^2$ and $5s5p$ levels are low lying and are much closer to the ground state than to the singly excited continuum, even for Z = 92. Between Z = 62 and 63 there is a crossing of the $^1S_0$ levels of the $5s^2$ (e) and $4f^2$ (j) configurations. The most serious interactions for $5s5p$ result from the plunging $4f5d$ configurations, which cross on Fig. 1 for $^1P_1$ at Z = 67–68 $(a$ and $f)$ and for ^3P_J at Z = 68–69 $(J$ = 2; b and $g)$, Z = 70–71 $(J$ = 1; c and $h)$, and Z = 71 $(J$ = 0; d and $i)$.

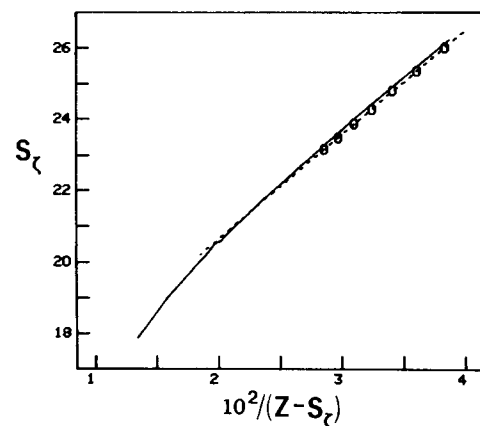The screening parameter reduction of the spin–orbit ener-

Fig. 2.   Spin–orbit screening parameter versus reciprocal screened charge. The solid line traces the MCDF calculations; the dashed line denotes a least-squares fit to the experimental values indicated by (0).

Table 3. Least-Squares-Adjusted Fitting Constants

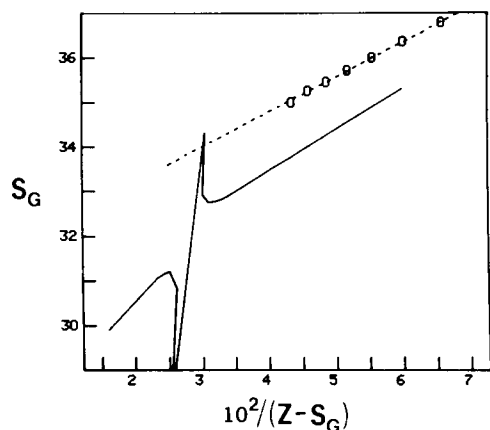| Quantity i	ϵ_i	a_i	b_i
ζ	—	14.786	291.93
G_{1A}	0.236	31.639	78.51
G_{1B}	0.261	31.163	83.16

Fig. 3.   Exchange screening parameter versus reciprocal screened charge. The solid line traces the MCDF calculations (with $\epsilon = 0$); the dashed line denotes a least-squares fit to the experimental values (with $\epsilon = 0.236$) indicated by (0).

gy both for the experimental data and for the theoretical calculations is shown in Fig. 2. To within experimental uncertainties, the experimental data follow a straight line on this plot, and the intercept and slope obtained from the least-squares fit (indicated by the dashed line) are given in Table 3. The theoretical calculations, however, exhibit a slight curvature on this plot that becomes more pronounced for $Z > 74$ (where the dashed line terminates). In the low-Z region at the upper right portion of the plot, the theoretical values overestimate the screening (hence underestimate the fine-structure splitting), but the discrepancy gradually decreases with increasing Z. In a similar study[13] for the ^2P states in the Cu isoelectronic sequence, it was observed that the experimental curve consists of two nearly linear regions, with a slight discontinuity in slope at about 30 stages of ionization. It is therefore concluded that for $Z \leq 74$ a satisfactory estimate of the spin–orbit energy in the Cd sequence is obtained using the linear fit to the experimental points shown in Fig. 2.

The screening parameter reduction of the Slater exchange energy G_{1A} for both the experimental data and the theoretical calculations is shown in Fig. 3. The reduction to G_{1B} is virtually indistinguishable from G_{1A} on such a plot, although their separate specification improves the predictive accuracy. The reduction of theoretical values for G_{1A} used $\epsilon = 0$ in Eq. (5), whereas the reduction of experimental values used $\epsilon = 0.236$, adjusted to optimize the linearity of the plot. The values of ϵ and the fitted slopes and intercepts for the reductions of both G_{1A} and G_{1B} are given in Table 3. In the regions where data exist, both the experimental and theoretical reductions in Fig. 3 appear as straight lines, although the theoretical values systematically underestimate the screening (and hence overestimate the singlet–triplet splitting). In the region $Z = 67$–71 where $5s5p$ and $4f5d$ levels cross, dramatic excursions from linearity occur, but beyond that region linearity is re-established with a different slope and intercept. Thus, outside the level crossing region, a linear extrapolation of the experimental data provides a better estimate of the exchange energy than do the MCDF calcula-

Table 4.   Predicted Energies for the $5s^2$–$5s5p$ Intervals in the Cd Isoelectronic Sequence (in cm^{-1})[a]

Z	Ion	$^1S_0$–$^3P_0$ Pr[b]	Ob–Pr	$^1S_0$–$^3P_1$ Pr[b]	Ob–Pr	$^1S_0$–$^3P_2$ Pr[b]	Ob–Pr	$^1S_0$–$^1P_1$ Pr[c]	Ob–Pr
52	Te+4	75 120	−10	78 032	−7	86 028	−22	111 693	+15
53	I+5	85 626	+40	89 231	+31	99 692	−6	127 443	−19
54	Xe+6	96 097	+43	100 419	+32	113 680	−7	143 275	−14
55	Cs+7	106 543	+27	111 606	+24	128 036	−5	159 316	+10
56	Ba+8	116 987	−3	122 812	0	142 818	−13	175 689	+22
57	La+9	127 440	−27	134 045	−26	158 068	+16	192 494	−13
58	Ce+10	138 025		145 425		173 939		209 809	−1
59	Pr+11	148 711		156 917		190 432		227 703	
60	Nd+12	159 537		168 560		207 620		246 251	
61	Pm+13	170 579		180 426		225 611		265 566	
62	Sm+14	182 318		192 994		244 922		286 171	
63	Eu+15	190 375		201 883		261 209		303 728	
64	Gd+16	202 894		215 236		282 652		326 421	
65	Tb+17	214 392		227 569		303 807		348 811	
66	Dy+18	225 617		239 628		325 462		371 688	
67	Ho+19	234 545		249 388		345 633		393 070	
68	Er+20	259 050		274 722		382 238		430 876	
69	Tm+21	265 643		282 142		401 832		451 665	
70	Yb+22	277 306		294 629		427 442		478 464	
71	Lu+23	289 740		307 882		454 816		507 024	
72	Hf+24	302 571		321 529		483 631		537 022	
73	Ta+25	315 726		335 495		513 864		568 435	
74	W+26	329 180		349 756		545 544		601 292	

[a] Where available, observed (Ob) and predicted (Pr) values are compared.
[b] Obtained from the fits of Table 3. Eqs. (1)–(6), and c below.
[c] Obtained by summing the corresponding column in Table 1 and the empirically fitted correction $280-1046Z + 42.75Z^2$.

tions. Near the level crossing region the linear extrapolation will not give reliable predictions, but theoretical estimates of isoelectronic level crossings are often shifted by one or more ions and can also be unreliable for a specific element. However, a comparison of the smoothed extrapolation with the results of future experimental investigations could be used to pinpoint these level crossings.

The screening parameterization described above specifies the relative separations of the levels of the $5s5p$ configuration, but to establish their positions relative to $5s^2$ an additional empirical extrapolation is necessary. I therefore studied the Z dependence of the difference between experimental measurements and MCDF calculations for the $5s^2$ $^1S_0$–$5s5p$ $^1P_1$ resonance transition. To within experimental accuracies, this difference is described by a least-squares fit to a quadratic polynomial in Z. Although this formulation is fully (rather than semi) empirical, it seems reasonable to assume that the major Z dependence is contained in the MCDF calculations and that the absolute error in this process will be small.

Combining this estimate for the singlet intervals with the screening parameterizations of ζ, G_{1A}, and G_{1B}, extrapolative predictions for $Z \leq 74$ were made. These predictions are presented and compared with available measurements in Table 4. Although a standard semiempirical extrapolation through as many as 34 stages of ionization would be only speculative, the use here of ab initio calculations to verify qualitative trends and of semiempirical parameterizations to quantify the predictions should provide reliability. The predictions in Table 4 should be of an accuracy far superior to that of purely ab initio calculations, and their reliability could be tested and improved if even a single measurement at a high stage of ionization could be made.

HOMOLOGOUS COMPARISONS

As discussed earlier, similar studies of $nsnp$ configurations were carried out previously for the Be, Mg, and Zn sequences. These systems can be subdivided into two different homologous groups. The Be, Mg, and Zn sequences (and highly ionized members of the 62-electron Sm sequence[14]) have two electrons outside a completely closed shell. The ns^2 and $nsnp$ configurations of the Zn, Cd, and Hg sequences have two electrons outside a closed nd^{10} subshell, which closes a shell only for the Zn sequence. Although the Zn, Cd, and Hg systems do not share the same plunging isoelectronic levels because of the variation in their open subshells, they do share a symmetry of core screening owing to this closed d subshell that can be exploited.

Figure 4 displays a further reduction of the spin–orbit and exchange-energy screening parameterizations. Data sources are Ref. 3 for the Zn sequence and Ref. 6 for the Hg sequence. The screening parameters were obtained as described above, but for plotting purposes a scaling procedure suggested by Edlén (Ref. 4, p. 184) was utilized. An effective number of screening electrons N was defined, and the quantities plotted were S/N and $N/(Z - S)$. It was found that if N is set equal to the total number of electrons ($N = 30, 48$, and 80 for the Zn, Cd, and Hg sequences), data for all three sequences occur along two straight lines: one each for the spin–orbit and exchange-energy reductions.

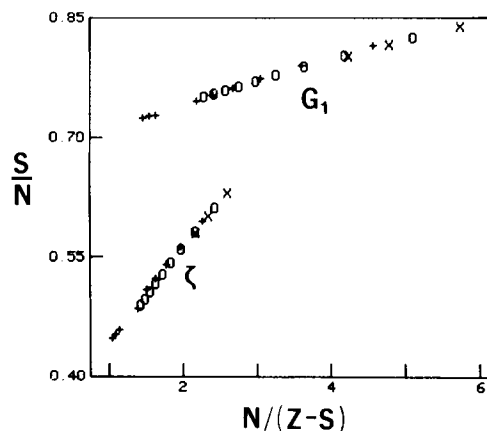Thus in a single plot Fig. 4 quantitatively describes the

Fig. 4. Reduced exchange and spin–orbit screening parameters versus the reduced reciprocal screened charge for the Zn (+), Cd (0), and Hg (X) isoelectronic sequences. N is the total number of electrons.

$nsnp$ intervals for three complete isoelectronic sequences (for $Z \leq 92$ this includes 121 different ions). Furthermore, these homologous alignments are sensitive to the value selected for N and do not occur unless all electrons (including the core and both valence electrons) are included in the count. Thus this exposition reveals large-scale regularities over substantial blocks of data that should also be exhibited by ab initio theories intended for use in these complex many-electron systems. In addition to possible theoretical insights, this linearity also has a direct application to the Hg sequence, since few data are currently available for that system.

CONCLUSIONS

Through the combined use of experimental data and ab initio calculations, the existence of linearizing systematizations in semiempirical parameterizations of the $5s5p$ configuration in the Cd sequence has been verified, and precise extrapolative isoelectronic predictions have been made to high stages of ionization. In addition, homologous regularities have been discovered that permit extensions of these analyses to the data-poor Hg isoelectronic sequence. Through formulations of this type it is possible that relativistic ab initio computational codes now available can be utilized to obtain the predictive accuracies required for high-resolution spectroscopic analysis.

ACKNOWLEDGMENTS

REFERENCES

1. B. Edlén, "A critical survey of the low configurations in Be I-like spectra," Phys. Scr. **20**, 129–137 (1979); "A critical compilation of energy levels in the configurations $2s^m2p^k$ ($m = 2, 1, 0$) of F I-, O I- and Be I-like spectra," Phys. Scr. **22**, 593–602 (1981); "Com-

parison of theoretical and experimental level values of the $n = 2$ complex in ions isoelectronic with Li, Be, O and F," Phys. Scr. **28,** 51–67 (1983).

2. L. J. Curtis and P. S. Ramanujam, "Isoelectronic wavelength predictions for magnetic-dipole, electric-quadrupole, and intercombination transitions in the Mg sequence," J. Opt. Soc. Am. **73,** 979–984 (1983).

3. L. J. Curtis, "Isoelectronic studies of the $4s4p\ ^3P_J$ energy levels in the Zn sequence," J. Opt. Soc. Am. B **2,** 407–410 (1985).

4. B. Edlén, "Atomic spectra," in *Handbuch der Physik*, S. Flügge, ed. (Springer-Verlag, Berlin, 1964), Vol. XXVII, pp. 80–220.

5. V. Kaufman and J. Sugar, National Bureau of Standards, Gaithersburg, Maryland 20899 (personal communication).

6. C. E. Moore, *Atomic Energy Levels—Volume III*, NSRDS-NBS 35 (U.S. Government Printing Office, Washington, D.C., reissued 1971).

7. K. Burns and K. B. Adams,"Energy levels and wavelengths of natural cadmium and of cadmium-114," J. Opt. Soc. Am. **46,** 94–99 (1956).

8. A. M. Crooker and Y. N. Joshi, "Spark spectra of tellurium," J. Opt. Soc. Am. **54,** 553–554 (1964).

9. J. A. O'Neill, E. H. Pinnington, K. E. Donnelly, and R. L. Brooks, "A study of the beam-foil spectrum of iodine from 400 and 1300 Å," Phys. Scr. **20,** 60–64 (1979).

10. E. J. Knystautas, J. Sugar, and J. R. Roberts, "New line classifications and energy levels in the triplet system of Xe VII," J. Opt. Soc. Am. **69,** 1726–1727 (1979).

11. I. P. Grant, Department of Theoretical Chemistry, 1 South Parks Road, Oxford OX1 3TG, UK (personal communication).

12. I. P. Grant, B. J. McKenzie, P. H. Norrington, D. F. Mayers, and N. C. Pyper, "An atomic multiconfigurational Dirac–Fock package," Comput. Phys. Commun. **21,** 207–231 (1980).

13. L. J. Curtis and R. R. Silbar, "Self-consistent core potentials for complex atoms: a semiclassical approach," J. Phys. B **17,** 4087–4101 (1984).

14. L. J. Curtis and D. G. Ellis, "Alkalilike spectra in the promethium isoelectronic sequence," Phys. Rev. Lett. **45,** 2099–2102 (1980).